Am J Physiol Renal Physiol 309: F318–F331, 2015.
First published June 24, 2015; doi:10.1152/ajprenal.00607.2014.

Ketamine-induced ulcerative cystitis and bladder apoptosis involve oxidative stress mediated by mitochondria and the endoplasmic reticulum

Keh-Min Liu,[1] Shu-Mien Chuang,[2] Cheng-Yu Long,[3] Yi-Lun Lee,[4,5] Chao-Chuan Wang,[1] Mei-Chin Lu,[6,7] Rong-Jyh Lin,[8] Jian-He Lu,[5] Mei-Yu Jang,[9] Wen-Jeng Wu,[9,10,11] Wan-Ting Ho,[10] and Yung-Shun Juan[5,9,10,11]

[1]*Department of Anatomy, College of Medicine, Kaohsiung Medical University, Kaohsiung, Taiwan;* [2]*Translational Research Center, Cancer Center, Department of Medical Research, Kaohsiung Medical University, Kaohsiung, Taiwan;* [3]*Department of Obstetrics and Gynecology, Kaohsiung Medical University Hospital, Kaohsiung, Taiwan;* [4]*Department of Urology, Chi-Shan Hospital, Department of Health, Executive Yuan, Kaohsiung, Taiwan;* [5]*Graduate Institute of Medical Science, Kaohsiung Medical University, Kaohsiung, Taiwan;* [6]*National Museum of Marine Biology and Aquarium, Pingtung, Taiwan;* [7]*Graduate Institute of Marine Biotechnology, National Dong Hwa University, Pingtung, Taiwan;* [8]*Department of Parasitology, College of Medicine, Kaohsiung Medical University, Kaohsiung, Taiwan;* [9]*Department of Urology, Kaohsiung Municipal Hsiao-Kang Hospital, Kaohsiung, Taiwan;* [10]*Department of Urology, College of Medicine, Kaohsiung Medical University, Kaohsiung, Taiwan; and* [11]*Department of Urology, Kaohsiung Medical University Hospital, Kaohsiung, Taiwan*

Submitted 12 November 2014; accepted in final form 16 June 2015

Liu K, Chuang S, Long C, Lee Y, Wang C, Lu M, Lin R, Lu J, Jang M, Wu W, Ho W, Juan Y. Ketamine-induced ulcerative cystitis and bladder apoptosis involve oxidative stress mediated by mitochondria and the endoplasmic reticulum. *Am J Physiol Renal Physiol* 309: F318–F331, 2015. First published June 24, 2015; doi:10.1152/ajprenal.00607.2014.—Ketamine abusers develop severe lower urinary tract symptoms. The major aims of the present study were to elucidate ketamine-induced ulcerative cystitis and bladder apoptosis in association with oxidative stress mediated by mitochondria and the endoplasmic reticulum (ER). Sprague-Dawley rats were distributed into three different groups, which received normal saline or ketamine for a period of 14 or 28 days, respectively. Double-labeled immunofluorescence experiments were performed to investigate tight junction proteins for urothelial barrier functions. A TUNEL assay was performed to evaluate the distribution of apoptotic cells. Western blot analysis was carried out to examine the expressions of urothelial tight junction proteins, ER stress markers, and apoptosis-associated proteins. Antioxidant enzymes, including SOD and catalase, were investigated by real-time PCR and immunofluorescence experiments. Ketamine-treated rats were found to display bladder hyperactivity. This bladder dysfunction was accompanied by disruptions of epithelial cadherin- and tight junction-associated proteins as well as increases in the expressions of apoptosis-associated proteins, which displayed features of mitochondria-dependent apoptotic signals and ER stress markers. Meanwhile, expressions of mitochondria respiratory subunit enzymes were significantly increased in ketamine-treated bladders. Conversely, mRNA expressions of the antioxidant enzymes Mn-SOD (SOD2), Cu/Zn-SOD (SOD1), and catalase were decreased after 28 days of ketamine treatment. These results demonstrate that ketamine enhanced the generation of oxidative stress mediated by mitochondria- and ER-dependent pathways and consequently contributed to bladder apoptosis and urothelial lining defects. Such oxidative stress-enhanced bladder cell apoptosis and urothelial barrier defects are potential factors that may play a crucial role in bladder overactivity and ulceration.

ketamine; mitochondria; endoplasmic reticulum; apoptosis; oxidative stress; urothelial barrier

KETAMINE, a noncompetitive *N*-methyl-D-aspartate (NMDA) receptor antagonist, is administered as an anesthetic drug for the treatment of chronic cancer pain and neuropathic pain. In recent years, the abuse of ketamine has dramatically increased worldwide, especially as a recreational drug in nightclubs and dance parties. Many studies have demonstrated that ketamine abusers develop severe lower urinary tract symptoms (10, 27, 42, 51, 55). Urinary signs and symptoms due to ketamine abuse/use have been reported to include suprapubic pain, urinary frequency, urinary urgency, urge incontinence, hematuria, and severe dysuria (11, 44, 51, 56). In addition, most clinical investigation findings in patients with ketamine-induced cystitis (49) include hydronephrosis, a small-capacity bladder, and papillary necrosis as well as urothelial inflammation, hemorrhages, and erythematous muscosa. In some cases of ketamine abuse, vesicoureteral reflux and ureteral obstruction also develop. Currently, no effective treatments are available for ketamine-induced cystitis (KIC) patients to either block or treat such ketamine-induced uropathy.

The bladder urothelium not only forms a tight barrier preventing noxious substances in urine from passing into the underlying stroma but is also involved in sensory mechanisms and can release chemical mediators (3). Previous studies have indicated that voiding function and the pathophysiology of interstitial cystitis/painful bladder syndrome (IC/PBS) and non-neurogenic overactive bladder are correlated with urothelial barrier dysfunction. Abnormal expression by IC/PBS bladder urothelial cell explants includes alterations in tight junction and adherens protein expression with decreases in occludin and zonula occludens (ZO)-1 and claudin-1, claudin-4, and claudin-8 expressions (33, 59). The decreased tight junction protein expression was reported to correlate with an increase in bladder urothelial permeability. In addition, in single cell electrophysiologic studies, explanted IC/PBS bladder urothelial cells were found to display a reduction in inward rectifying K^+ current with conductance of the Kir2.1 channel (23, 53) and an enhancement in sensitivity to carbachol, suggesting that muscarinic signaling may also be abnormally regulated in IC/BPS (23). The barrier function of the urothelium might

Address for reprint requests and other correspondence: Y.-S. Juan, Dept. of Urology, College of Medicine, Kaohsiung Medical Univ., 100 Shih-Chuan 1st Road, Sanmin District, Kaohsiung City 807, Taiwan (e-mail: juanuro@gmail.com).

Table 1. *Primer sequences used in real-time quantitative PCR*

Sequence Number	Gene Name	Primer Sequences		Accession Number	Melting Temperature, °C
		Forward	Reverse		
1	Mn-SOD	5′-AAGGAGCAAGGTCGCTTACA-3′	5′-ACACATCAATCCCCAGCAGT-3′	NM017051.2	59
2	Cu/Zn-SOD	5′-GGTGGTCCACGAGAAACAAG-3′	5′-CAATCACACCACAAGCCAAG-3′	NM017050.1	58
3	Catalase	5′-GAATGGCTATGGCTCACACA-3′	5′-CAAGTTTTTGATGCCCTGGT-3′	NM012520.2	59
4	β-Actin	5′-ATCTCCTTCTGCATCCTGTCGGCAAT-3′	5′-CATGGAGTCCTGGCATCCACGAAAC-3′	NM007393	59

also play an important role in the pathophysiology of KIC. Despite these advances, the etiological cell signaling and pathophysiological mechanisms of the bladder urothelium and voiding dysfunction in KIC patients remain unsettled.

Several pathophysiological conditions in the urinary bladder, e.g., bladder outlet obstruction (41, 43, 48), ischemia-reperfusion (19, 57) and inflammation (2, 7, 9), are characterized by the formation of ROS. Studies showed oxidative stress may reduce detrusor contractility by the damage to the muscarinic receptors (2, 18). The bladder urothelium and suburothelium can be targets for ROS release from inflammatory cells. Some studies have indicated that oxidative stress induced by H_2O_2 activates capsaicin-sensitive C-fiber afferent pathways mediated via stimulation of the cytochrome *c* oxidase (COX) pathway, thereby inducing detrusor overactivity (45). The elevated ROS can further cause damage to biological molecules, such as DNA, resulting in gene mutations (38).

There are two major intracellular organelles that generate ROS and signal apoptosis, i.e., mitochondria and the endoplasmic reticulum (ER) (47, 54). The mitochondrion is a key venue for cellular metabolism and serves as the powerhouse of the cell. In consequence, mitochondrial content is influenced by cellular energy demand. In the oxidative phosphorylation cycle, sequential oxidation and reduction reactions take place in a chain of multiprotein complexes. The mitochondria-mediated apoptotic pathway initiates signaling via increases in mitochondrial membrane permeability, which promotes the release of cytochrome *c* and the activation of caspases (22). The ATP receptor P2X3, when constitutively knocked out, has been reported to result in a hyposensitive bladder (16). A recent study (46) using the KIC mouse model showed an enhancement in noncholinergic contractions and P2X1 receptor expression in ketamine-induced bladder dysfunction. The ER-mediated pathway is triggered by ER stress, which leads to a proapoptotic unfolded protein response, including the induction of CCAAT/enhancer-binding protein homologous protein (CHOP) and 78-kDa glucose-regulated protein (GRP78) (25, 34).

Due to the lack of specific biomarkers, most KIC patients are diagnosed late after the exclusion of other diseases and suffer irreversible bladder damage by the time of diagnosis. A number of theories for the development of KIC have been proposed (10, 11), including *1*) a direct toxic effect of ketamine or its metabolites on bladder interstitial cells, *2*) microvascular changes in the bladder by ketamine and/or its metabolites, and *3*) indirect effects of ketamine by causing an autoimmune reaction against the bladder urothelium and submucosa. In extension of our previous investigations of bladder dysfunction and KIC (13, 27), the major aims of the present study were to evaluate whether ketamine enhances mitochondrial and ER oxidative stress, induces apoptosis, and causes damage of the bladder in a rat KIC model. We hypothesized that ketamine addiction enhanced bladder oxidative stress, urothelial injury,

Table 2. *General characteristics, biochemistry, and urodynamic parameters for the different experimental groups*

	Control Group	K14D Group	K28D Group
Number of rats	16	16	16
General characteristics			
Body weight, g	266.0 ± 37.2	260.0 ± 31.6	267.0 ± 36.8
Bladder weight, mg	150.0 ± 8.0	154.0 ± 18.0	188.0 ± 26.0*
Urodynamic parameters			
Frequency, number of voids/1 h	3.2 ± 0.5	6.0 ± 1.8†	11.6 ± 2.5†
Peak micturition pressure, cmH_2O	32.3 ± 4.4	44.6 ± 5.7*	52.7 ± 6.1†
Voided volume, ml	1.8 ± 0.3	1.3 ± 0.4*	0.7 ± 0.2†
Number of nonvoiding contractions between micturition, number of nonvoiding contractions/1 h	0	0	3.4 ± 0.6†
Water intake, ml/24 h	30.6 ± 3.5	31.0 ± 5.3	28.4 ± 5.8
Urine output, ml/24 h	26.5 ± 3.5	24.5 ± 4.2	18.2 ± 3.9*
Serum parameters			
Ketamine concentration, ng/ml	ND	ND	ND
Norketamine concentration, ng/ml	ND	ND	ND
Urine parameters			
Ketamine concentration, ng/ml	ND	1406.0 ± 241.0†	1668.0 ± 225.6†
Norketamine concentration, ng/ml	ND	30016.0 ± 1161.4†	33720.2 ± 1262.7†
Urine protein/creatinine	0.51 ± 0.13	1.06 ± 0.25†	1.38 ± 0.32†
Creatinine clearance rate	1.12 ± 0.16	1.02 ± 0.15	0.82 ± 0.13†

Values are means ± SD. Sprague-Dawley rats were distributed into three groups that received intraperitoneal injections of saline (0.5 ml) for 14 or 28 days (control group) or ketamine (25 $mg \cdot kg^{-1} \cdot day^{-1}$) daily for a period of 14 days (K14D group) or 28 days (K28D group). ND, not detected. *$P < 0.05$ and †$P < 0.01$ vs. the control group.

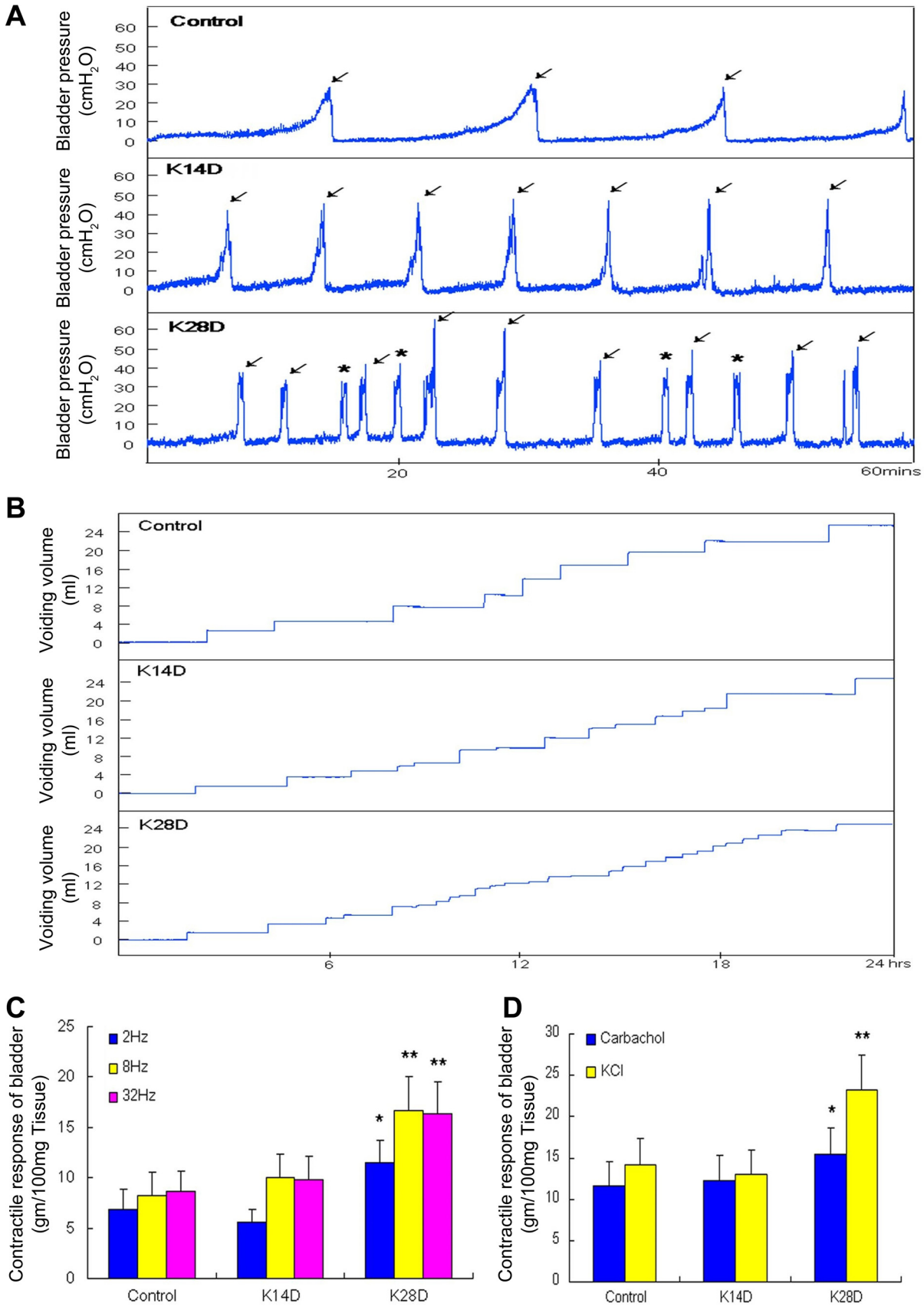

extracellular matrix remodeling, and apoptosis, which subsequently attributed to bladder dysfunction.

MATERIALS AND METHODS

Animals and ketamine administration. Experiments were performed on 48 adult female Sprague-Dawley (20) rats (Animal Center of BioLASCO, Taipei, Taiwan) that weighed between 200 and 250 g. Forty-eight Sprague-Dawley rats were distributed into three groups that received intraperitoneal injections of saline (0.5 ml) for 14 or 28 days (control group) or ketamine (25 $mg \cdot kg^{-1} \cdot day^{-1}$) daily for a period of 14 days (K14D group) or 28 days (K28D group). This study was approved by the Animal Care and Treatment Committee of Kaohsiung Medical University (Institutional Animal Care and Use Committee permit no 101136). All experiments were conducted in strict accordance with recommendations in the National Institutes of Health *Guide for the Care and Use of Laboratory Animals*, and all efforts were made to minimize animal stress/distress.

Physical indicators for bladder function. As previously described (13, 40), rats were placed in individual KDS-TL380 metabolic cages with a MLT0380 transducer (AD Instruments, Colorado Springs, CO). Micturation frequency and the volume of urine output were recorded for 3 days, and an average value was determined. Twenty-four-hour urine was collected to measure protein and creatinine levels. Blood (serum) creatinine was also determined. The ratio of protein to creatinine in urine and the creatinine clearance rate (CCr) were calculated.

Cystometrogram experiments. Cystometrograms (CMGs) were carried out according to previously described methods (6, 29, 39). The bladder was infused with 0.9% NaCl (normal saline) at a steady rate (0.08 ml/min). CMGs were recorded until the bladder pressure was stable, and reproducible micturation cycles were then recorded for 1 h. Pressure and force signals were amplified (ML866 PowerLab, AD Iinstruments) and recorded on a chart recorder for computer data analysis (Labchart 7, AD IInstruments; Windows 7 system). The CMG parameters recorded included peak micturation pressure, bladder volume, and frequency of nonvoiding contractions (without urine leakage during bladder infusion). A voiding contraction was defined as an increase in bladder pressure that resulted in urine loss. Peak micturation pressure was the maximum pressure during micturation as observed in CMGs (24).

Bladder strip preparation and contractile responses. The contractile response was characterized in three ways (field stimulation, carbachol, and KCl), making it possible to determine if contractile defects were related to synaptic transmission, receptor responses, or smooth muscle dysfunction. The bladder square after longitudinal dissection was $\sim 2.0 \times 2.0$ cm^2 in a 250-g rat. After the bladder had been weighed, at best four longitudinal strips of 0.5×2.0 cm^2 could be prepared for each rat. Three longitudinal strips measuring 0.5×2.0 cm^2 were obtained from the bladder dome to the trigone area including both the muscle and mucosal layers. Contractile responses were measured as previously described (12, 30). Briefly, each whole layer bladder strip was mounted in a separate 15-ml bath containing Tyrode solution (124.9 mM NaCl, 2.6 mM KCl, 23.8 mM $NaHCO_3$, 0.5 mM $MgCl_2$, 0.4 mM NaH_2PO_4, 1.8 mM $CaCl_2$, and 5.5 mM dextrose), which was equilibrated with a mixture of 95% O_2 and 5% CO_2. An initial resting tension of 2 g was applied for 30 min, and contractile responses were recorded isometrically using a force-displacement transducer. The maximal response was determined sequentially for electrical field stimulation (EFS; 2, 8, and 32 Hz), carbachol (20 μM), and KCl (120 mM) (32).

Ketamine and metabolites assay in urine and serum by HPLC. Urine was collected after the last ketamine intraperitoneal injection for a period of 24 h. The rat was then euthanized the next day (24 h) after ketamine injection. One milliliter of blood was obtained from the rat tail to analyze serum ketamine and norketamine. Urine was also collected by the metabolic cage on the same day. Concentrations of ketamine and norketamine in urine and serum were determined by HPLC (13, 17, 49). After purification by liquid-liquid extraction using ethyl ether, urine and serum samples underwent chromatography on a reversed-phase column, and ketamine and norketamine were detected at 200 nm by ultraviolet spectrophotometry.

Histological experiments. Experimental rats were perfused with 0.9% normal saline solution through the left ventricle. The bladders were then removed, cut open, and further fixed overnight. Tissue samples were embedded in paraffin blocks with the same area in the different groups, and serial sections of 5 μm thick were obtained. Deparaffinized sections were stained with Masson's trichrome stain (Masson's Trichrome Stain Kit HT15, Sigma, St. Louis MO). A standard Masson's trichrome staining procedure was followed (13, 29). The standard Masson's trichrome stained the connective tissue in blue and detrusor smooth muscle (DSM) in red. Histology slides were reviewed by two independent pathologists.

Apoptotic cell staining by TUNEL assay. To detect cells undergoing apoptosis, tissue sections were processed by a TUNEL assay using an in situ cell death detection kit (Roche, Pleasanton, CA). DNA strand breaks were identified by labeling free 3′-OH with fluorescence in dUTP plus terminal transferase. The number of TUNEL-positive cells in 10 randomly selected nonoverlapping fields of ×400 magnification in the bladder was calculated and compared between the various groups. In each experiment, negative controls with label solution (without terminal transferase) instead of the TUNEL reaction mixture were used to elucidate nonspecific immunostaining.

Immunofluorescence experiments of the expression and localization of the bladder urothelial barrier, ER stress, and antioxidant proteins. Immunostaining was performed according to previously published methods (13). Sections were then doubly stained with primary antibody to claudin-4 (Invitrogen, Camarillo, CA, mouse monoclonal IgG1, 1:100, clone 3E2C1, catalog no. 32-9400), E-cadherin (Proteintech, Chicago, IL, rabbit polyclonal IgG, 1:100, catalog no. 20874-1-AP), GRP78 (Proteintech, rabbit polyclonal IgG, 1: 50, catalog no. 11587-1-AP) and CHOP (Abcam, Cambridge, MA, mouse monoclonal IgG2b, 1:100, clone 9C8, catalog no. ab11419) overnight and then incubated with secondary antibody (Invitrogen, goat anti-mouse or anti-rabbit, 1:800) conjugated to FITC for claudin-4 and GRP78 and to rodamine for E-cadherin and CHOP followed by 4′,6-diamidino-2-phenylindole (DAPI; Invitrogen, 500 μg/ml, 1:2,000) for 15 min. Tissue sections were also stained with Mn-SOD (SOD2; Abcam, mouse monoclonal IgG1, 1:100, clone 2A1, catalog no. ab16956), Cu/Mn-SOD (SOD1; Abcam, rabbit monoclonal IgG, 1:100, clone EP1727Y, catalog no. ab51254), and catalase (Abcam, rabbit polyclonal IgG, 1:100, catalog no. ab16731) antibodies overnight and then incubated with secondary antibody conjugated to FITC for SOD2 and to rodamine for SOD1 and catalase. Ten randomly selected nonoverlapping fields of ×400 magnification were collected,

Fig. 1. Effects of ketamine administration on bladder cystometric parameters, voiding behavior, and contractile responses. *A*: cystometry recordings illustrating micturation pressure and voiding frequency, including voiding contractions (arrows) and nonvoiding contractions (*). *B*: effect of ketamine administration on voiding behavior. Representative traces show micturation frequency and urine volume in rats that received intraperitoneal injections of saline (0.5 ml) for 14 or 28 days (control group) or ketamine (25 $mg \cdot kg^{-1} \cdot day^{-1}$) daily for a period of 14 days (K28D group) or 28 days (K28D group) in 24-h intervals. Values are means ± SD for $n = 16$. *C* and *D*: bladder contractile responses to electrical field stimulation (*C*) or carbachol and KCl (*D*) for the three different groups. Values are means ± SD for $n = 8$. $*P < 0.05$ and $**P < 0.01$ vs. the control group.

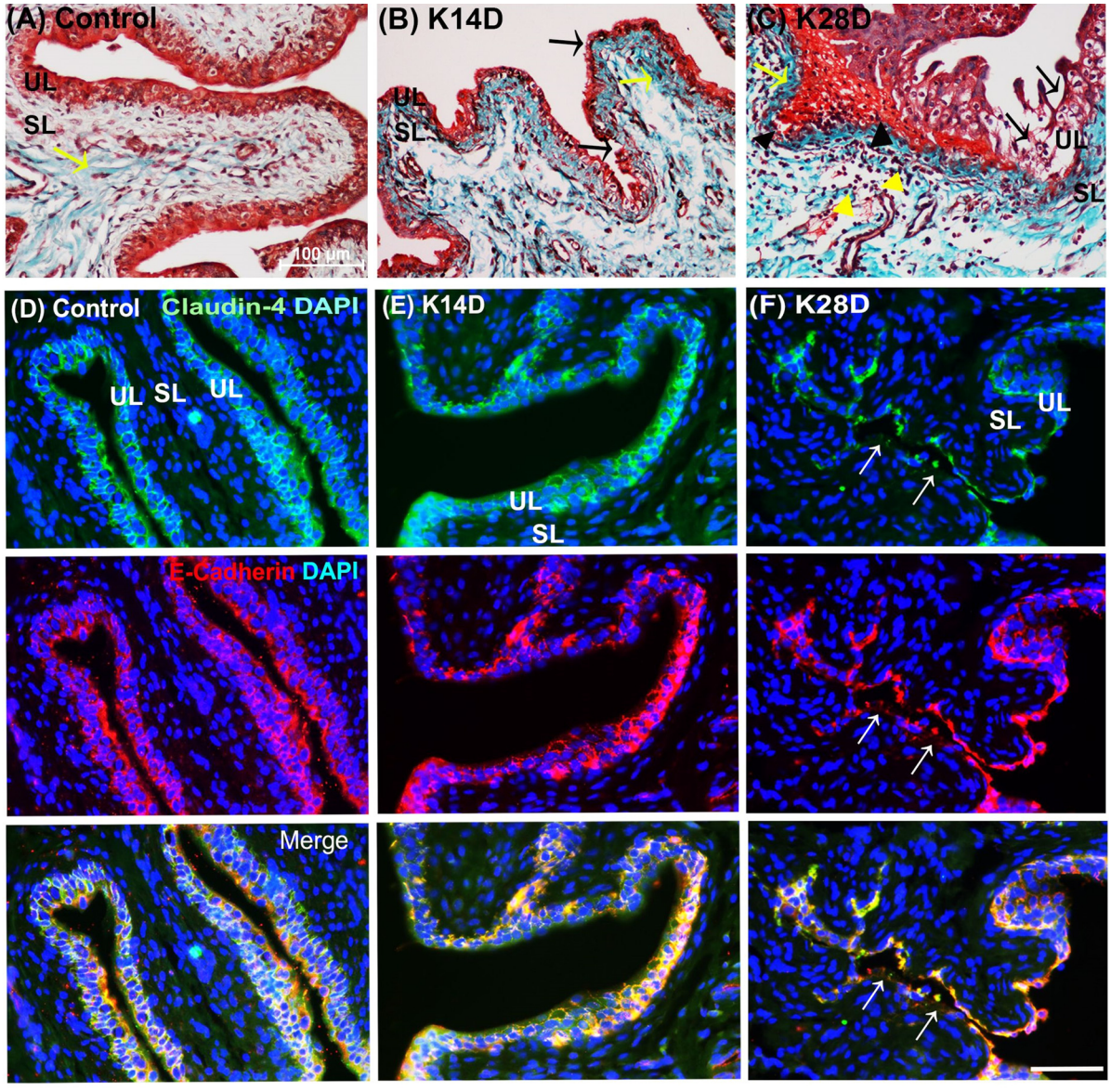

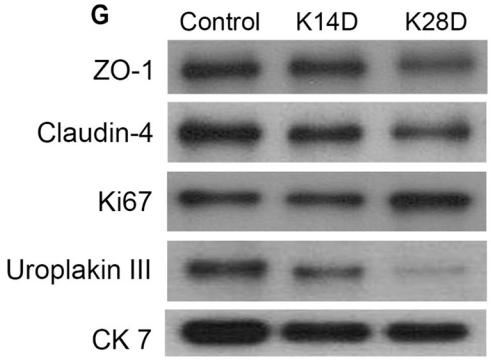

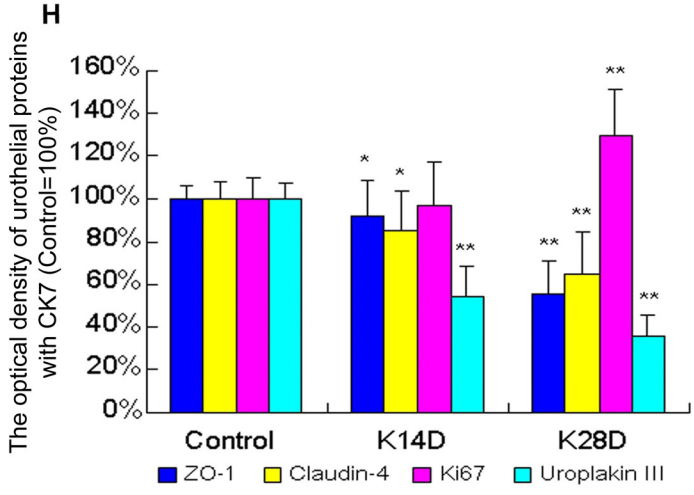

and slides were reviewed by two different pathologists. In each experiment, negative controls without primary antibody were performed to elucidate nonspecific immunostaining.

Protein isolation and Western blot analysis. According to previously described methods (29), frozen tissue samples of the bladder were homogenized on ice in buffer [50 mM Tris (pH 7.5) and 5% Triton X-100] containing halt protease inhibitor cocktail (Pierce, Rockford, IL) at 100 mg/ml. Protein (30 μg) from the bladders was loaded onto SDS-PAGE gels and transferred to polyvinylidene fluoride membranes (Immobilon-P, Millipore). Immobilon-P membranes were incubated with primary antibodies to Ki67 (Abcam, rabbit monoclonal IgG, 1: 1,000, clone SP6, catalog no. ab16667), uroplakin III [Abcam, mouse monoclonal IgG1, 1:1,000, molecular weight (MW): 32 kDa, clone SFI-1, catalog no. ab78196], nitrotyrosine (Enzo, Farmingdale, NY, mouse monoclonal IgG1, 1:1,000, MW: 62 kDa, clone NOY-7A5, catalog no. ALX-804-208), 2,4-dinitrophenol (DNP; Bethyl, Montgomery, AL, goat polyclonal IgG, 1:1,000, MW: 110 kDa, catalog no. A150-117A), cytochrome *c* (Abcam, mouse monoclonal IgG, 1:1,000, MW: 15 kDa, clone 7H8.2C12, catalog no. ab13575), caspase-3 (Abcam, rabbit polyclonal IgG, 1:500, MW: 32 kDa, catalog no. ab44976), caspase-8 (Cell Signaling, Danvers, MA, rabbit polyclonal IgG, 1:1,000, MW: 57 kDa, clone D35G2, catalog no. 4790), caspase-9 (Millipore, rabbit monoclonal IgG, 1:2,000, MW: 46 kDa, catalog no. 04-443), poly(ADP-ribose) polymerase (PARP; Cell Signaling, rabbit monoclonal IgG, 1:1,000, MW: 116 kDa, catalog no. 9532), Bcl-2 (Cell Signaling, rabbit monoclonal IgG, 1:1,000, MW: 26 kDa, clone 50E3, catalog no. 2870), claudin-4 (Invitrogen, mouse monoclonal IgG1, 1:1,000, MW: 225 kDa, clone 3E2C1, catalog no. 32-9400), ZO-1 (Invitrogen, rabbit polyclonal IgG, 1:1,000, MW: 225 kDa, catalog no. 40-2200), caspase-12 (Abcam, rabbit polyclonal IgG, 1:1,000, MW: 55 and 36 kDa, catalog no. ab18766), GRP78 (Proteintech, rabbit polyclonal IgG, 1:1,000, MW: 78 kDa, catalog no. 11587-1-AP), CHOP (Abcam, mouse monoclonal IgG2b, 1:1,000, MW: 31 kDa, clone 9C8, catalog no. ab11419), NADH dehydrogenase (ubiquinone) Fe-S protein 3 (NDUFS3; Abcam, mouse monoclonal IgG1, 1:1,000, MW: 30 kDa, clone 3F9DD2, catalog no. ab110246), succinate dehydrogenase complex subunit A (SDHA; Abcam, mouse monoclonal IgG1, 1:1,000, MW: 70 kDa, clone 2E3GC12FB2AE2, catalog no. ab14715), ubiquinol-cytochrome *c* reductase core protein II (UQCRC2; Abcam, mouse monoclonal IgG1, 1:1,000, MW: 48 kDa, clone 13G12AF12BB11, catalog no. ab14745), COX-2 (Cayman, Ann Arbor, MI, mouse monoclonal IgG1, 1:1,000, MW: 72 kDa, clone CX 229, catalog no. 160112), ATPB (Abcam, mouse monoclonal IgG1, 1:1,000, MW: 52 kDa, clone 3D5, catalog no. ab14730), cytokeratin 7 (Abcam, mouse monoclonal IgG1, 1:200, MW: 55 kDa, clone RCK105, catalog no. ab9021), and β-actin (Millipore, mouse monoclonal IgG2b, 1:1,000, MW: 43 kDa, clone C4, catalog no. MAB1501). The proliferation marker (Ki67), differentiated urothelial marker (uroplakin III), oxidative stress markers (DNP and nitrotyrosine), tight junction (claudin-4 and ZO-1), adhesion protein (E-cadherin), proapoptotic (cytochrome *c*, caspase-3, caspase-8, caspase-9, and PARP), antiapoptotic (Bcl-2), ER markers (GRP78, CHOP, and caspase-12) and protein expressions of mitochondrial respiratory enzyme complexes (NDUFS3, SDHA, UQCRC1, COX-2, and ATPB) were normalized with β-actin or cytokeratin 7 as an epithelial marker. In each experiment, negative controls were also done without primary antibody.

Real-time quantitative PCR. The expression of antioxidant enzymes (Cu/Zn-SOD, Mn-SOD, and catalase) involving oxidative stress was analyzed using real-time quantitative RT-PCR as previously described (50). Experimental rats were perfused with 0.9% saline solution, and RNA samples were isolated from rat bladders. RNA samples with the ratios between the absorbance at 260 and 280 nm exceeding 1.7 were stored at −80°C for further analysis. An aliquot of 5 μg RNA was used to generate cDNA. The SYBR green I kit (Takara Biotechnology) was used; all primers are shown in Table 1. The specificity of products generated for each set of primers was examined for each fragment with the use of a melting curve and gel electrophoresis. Relative expression levels for each targeted gene were normalized by subtracting the corresponding β-actin threshold cycle (C_T) values using the $\Delta\Delta C_T$ comparative method (58). A total of eight samples for each group were used, and each sample was run in triplicate for real-time PCR.

Statistical analysis. ANOVA followed by the Bonferroni test and two-way ANOVA for individual comparisons were conducted for the above experiments. Means, SDs (20), and *P* values were calculated for triplicate experiments. Student's *t*-test was used to calculate *P* values for comparison. The significant level was set at a *P* value of <0.05.

RESULTS

Effects of ketamine treatment on cystometric parameters and voiding behavior. CMG parameters, including peak micturation pressure, micturation frequency, and voiding and nonvoiding contractions, are shown in Table 2. Ketamine treatment increased bladder hyperactivity with increases in voiding contraction (arrows), nonvoiding contraction (asterisks), peak micturation pressure, and micturation frequency (Fig. 1*A*). There were significant increases in micturation frequency (3.62-fold) as well as nonvoiding contraction frequency and peak micturation pressure (1.63-fold). In contrast, there was a decrease in the micturation interval and bladder volume (0.38-fold) in the K28D group compared with those in control rats (Table 2). In addition, tracing analysis of voiding behavior using metabolic cages revealed an increase in micturation frequency and a decrease in voiding volume in both K14D and K28D groups compared with the control group (Fig. 1*B* and Table 2). These results demonstrate that ketamine treatment caused significant bladder storage dysfunction.

Effects of ketamine treatment on the bladder contractile response. Contractile responses of bladder strips in response to EFS (2, 8, and 32 Hz), carbachol (20 μM), or KCl stimulation are shown in Fig. 1, *C* and *D*. The K28D group exhibited stronger contractile responses to EFS at 2, 8, and 32 Hz than the control and K14D groups. Similar observations were found in response to carbachol and KCl. Therefore, ketamine admin-

Fig. 2. Ketamine administration increased bladder fibrosis and disrupted the urothelial barrier. *A–C*: representative microphotographs of the control (*A*), K14D (*B*), and K28D (*C*) groups with Masson's trichrome stain. Blue-stained collagen and red-counterstained detrusor smooth muscle (DSM) are highlighted in each image. In the control group (*A*), there were three to five layers of the urothelial layer (UL) and only sparse collagen distributed in the suburothelial layer (SL). In the K14D group (*B*), bladder tissues demonstrated a thinning urothelium (black arrow) and increased interstitial fibrosis (yellow arrow). The K28D group (*C*) showed a denuded urothelial mucosa (black arrow), erythrocyte debris under the urothelium (black arrowhead), mononuclear cell infiltration (yellow arrow), and increased bladder fibrosis (yellow arrow). *D–F*: expressions of E-cadherin and claudin-4 proteins in bladder tissue as demonstrated by immunofluorescence stain. Claudin-4 (22) and E-cadherin (red) were colabeled in the bladder UL. *F*: expressions of these proteins were costained in the defective and thinnng urothelium (arrow) in the K28D group. Scale bar = 100 μm. *G*: expression levels of tight junction protein [claudin-4 and zonula occludens (ZO)-1], proliferation marker (Ki67), and urothelial differentiation marker (uroplakin III) were determined in the different groups by Western blot analysis. *H*: quantification of these proteins to cytokeratin 7 (CK7). Results were normalized to the control group (equal to 100%). Values are means ± SD for $n = 8$. $^*P < 0.05$ and $^{**}P < 0.01$ vs. the control group.

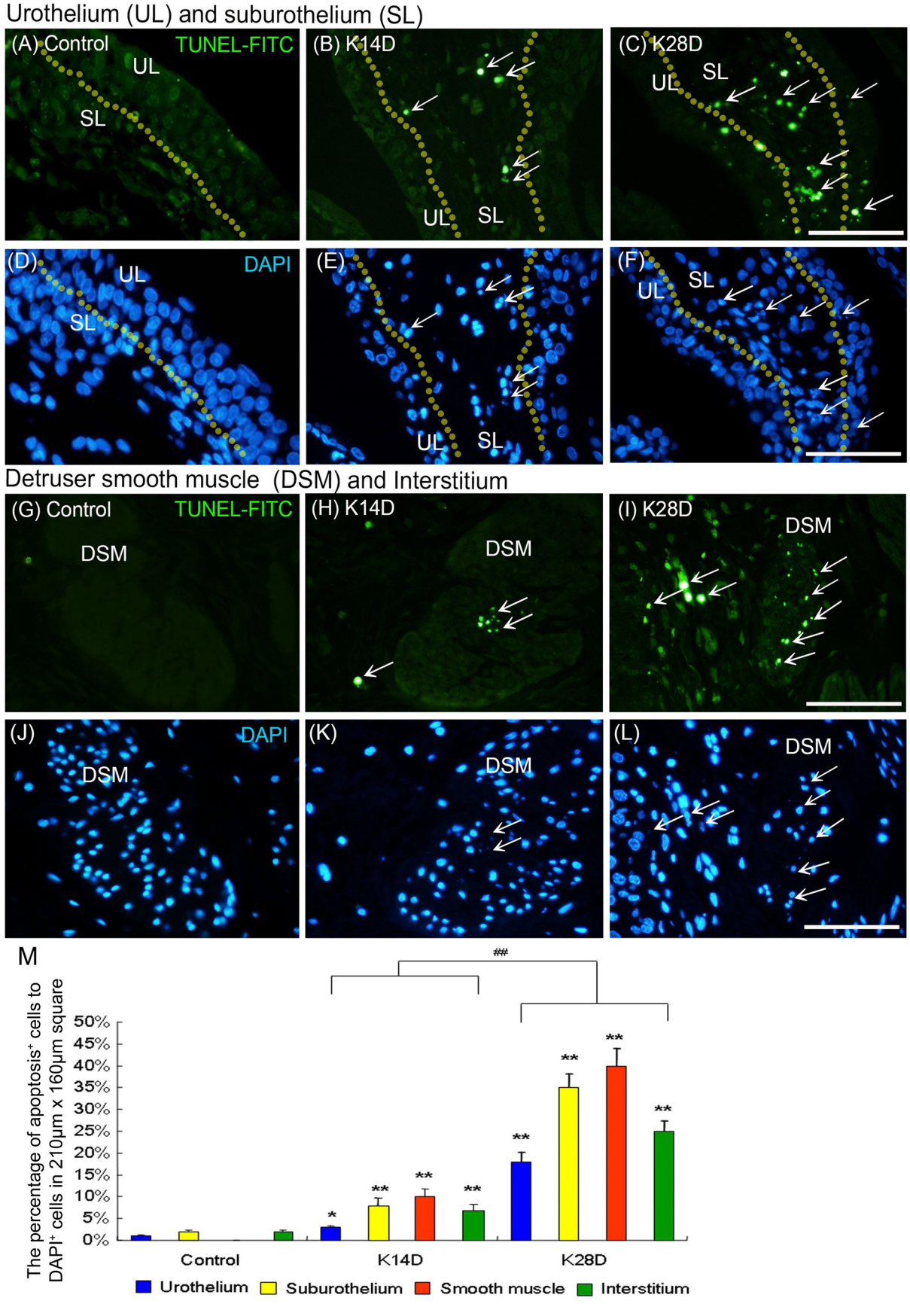

istration strongly induced bladder contractile in response to these stimulations.

Concentrations of ketamine and its metabolites in urine and serum. Ketamine is metabolized by the liver to norketamine (primary metabolite) and is excreted in urine (49). Concentrations of ketamine and norketamine in serum and urine are shown in Table 2. In the control group, concentrations of ketamine and norketamine were undetectable in both urine and serum. In contrast, concentrations of urine ketamine and norketamine were 1,406.0 ± 241.0 and 30,016.0 ± 1,161.4 ng/ml in the K14D group and 1,668.0 ± 225.6 and 33,720.2 ± 1,262.7 ng/ml in the K28D group, respectively. These results show that ketamine-treated rats produced significant amounts of ketamine and norketamine in urine but were not detectable in serum, suggesting that the metabolism of ketamine was quick and that the rat liver could clear ketamine within 1 day. Comparisons of these results revealed that the toxic effects of ketamine in the urinary bladder were derived from not only ketamine but also its primary metabolite, norketamine.

Physical characteristics of ketamine-associated bladder damage and renal function suppression. General characteristics of rats after ketamine treatment, including body weight, bladder weight, water intake, and urine output, are shown in Table 2. The ratio of urine protein to creatinine and CCr were also calculated to evaluate renal function. There were no significant differences in body weight, bladder weight, CCr, water intake, and urine output between the control and K14D groups. However, the K28D group showed significant increases in bladder weight and the ratio of urine protein to creatinine but a decline in CCr compared with the control group (Table 2). These findings demonstrate that ketamine treatment resulted in not only bladder but also renal dysfunction.

Histological features of ketamine-associated bladder damage and interstitial fibrosis. Histological features of ketamine-associated bladder damage are shown in Fig. 2. In the control group, there were three to five layers of the urothelium and only sparse collagen (blue color, yellow arrow) in the suburothelium (Fig. 2*A*). In the K14D group, bladder tissues were characterized by a thinning urothelium (black arrow) and increased interstitial fibrosis (yellow arrow; Fig. 2*B*). Moreover, the morphology of the K28D group (Fig. 2*C*) was characterized by an ulcerated urothelium (black arrow), erythrocyte accumulation (hemorrhages; black arrowhead), mononuclear cell infiltration (yellow arrowhead), and increased interstitial fibrosis (yellow arrow) between DSM bundles.

Ketamine-induced alterations in urothelial junction-associated protein expression. The urothelial distribution of claudin-4 (tight junction protein) and E-cadherin (adhesion protein) are also shown in Fig. 2. In the control group, claudin-4 and E-cadherin overlapping immunolabeling was widely distributed in intercellular junctions of the urothelial layer, whereas the suburothelial layer showed no immunoreactivity for either claudin-4 or E-cadherin (Fig. 2*D*). Moreover, the immunolabeling of claudin-4 and E-cadherin in the K14D group was restricted to the thin urothelium (Fig. 2*E*). However, in the K28D group, the immunolabeling of claudin-4 and E-cadherin was much lower and restricted to the thinner and disrupted urothelium (arrows; Fig. 2*F*). Furthermore, tight junction proteins (claudin-4 and ZO-1) and the differentiated marker of umbrella cells of the outer urothelium (uroplakin III) in the K14D and K28D groups were significantly less compared with the control group (Fig. 2, *G* and *H*). However, the proliferation marker (Ki67) in the K28D group was significantly increased compared with the control group (Fig. 2, *G* and *H*). These results demonstrate that ketamine administration for 28 days decreased urothelial barrier-associated protein expressions, which might attribute to urothelial lining defects during the inflammation process of KIC.

Ketamine-induced bladder cell apoptosis. The results of TUNEL staining to detect degenerated apoptotic cells in the bladder after ketamine administration are shown in Fig. 3. The number of apoptotic cells in the urothelial and suburothelial layers was significantly higher in the K14D and K28D groups than in the control group (Fig. 3, *A–F*). Similar observations were found for the number of apoptotic cells in the DSM and interstitium (Fig. 3, *G–L*). In the control group, the percentage of TUNEL-positive to DAPI-positive cells was 0.9 ± 0.1% in the urothelial layer and 2.3 ± 0.3% in the suburothelial layer (Fig. 3, *A*, *D*, and M), but almost no TUNEL-positive cells were found in the DSM and interstitium (Fig. 3, *G*, *J*, and *M*). In contrast, after 14 days ketamine treatment, the percentage of TUNEL-positive to DAPI-positive cells was significantly increased to 3.5 ± 0.4% in the urothelial layer and 7.6 ± 1.3% in the suburothelial layer (Fig. 3, *B*, *E*, and *M*) and 9.8 ± 1.5% in the DSM and 7.2 ± 1.4% in the interstitium (Fig. 3, *H*, *K*, and *M*). Moreover, after 28 days ketamine treatment, the percentage of TUNEL-positive to DAPI-positive cells was 17.2 ± 1.8% in the urothelial layer and 34.4 ± 4.7% in the suburothelial layer (Fig. 3, *C*, *F*, and *M*) and 38.6 ± 5.5% in the DSM and 25.3 ± 2.7% in the interstitium (Fig. 3, *I*, *L*, and *M*). Apoptosis was significantly observed in the bladder urothelium, suburothelium, DSM, and interstitium after 28 days ketamine injection, revealing that ketamine treatment induced bladder apoptosis.

Mitochondria- and ER-elicited bladder apoptosis after ketamine injection. To evaluate whether ketamine-induced apoptosis is mediated through mitochondrial dysfunction pathways, the effect of ketamine on the expressions of proapoptosis markers for mitochondria was examined. As shown in Fig. 4, *A* and *C*, expression of the antiapoptotic protein Bcl-2 in bladder tissues was significantly decreased in the K14D and K28D groups. In contrast, expressions of the proapoptotic proteins cytochrome *c*, caspase-3, caspase-8, caspase-9, and PARP were significantly increased in the K28D group. Moreover, the involvement of ER stress signaling triggered by ketamine treatment was evaluated based on ER chaperone GRP78, ER-associated apoptosis protein CHOP, and caspase-12. As shown in Fig. 4, *B* and *D*, ketamine increased expression levels of caspase-12, GRP78, and CHOP in the K14D and

Fig. 3. Ketamine-induced bladder cell apoptosis as evaluated by the TUNEL assay. *A–L*: apoptosis of bladder cells was detected by TUNEL (FITC, green) and 4′,6-diamidino-2-phenylindole (DAPI) staining (blue) for the UL and SL (*A–F*) and for the DSM and interstitium (*G–L*). There were increases in TUNEL-positive nuclei (white arrows) in the bladders of K14D and K28D rats. Scale bar = 100 μm. *M*: quantification of the number of apoptotic cells in the UL, SL, DSM, and interstitium. Scale bar = 100 μm. Values are means ± SD for $n = 8$. *$P < 0.05$ and **$P < 0.01$ vs. the control group.

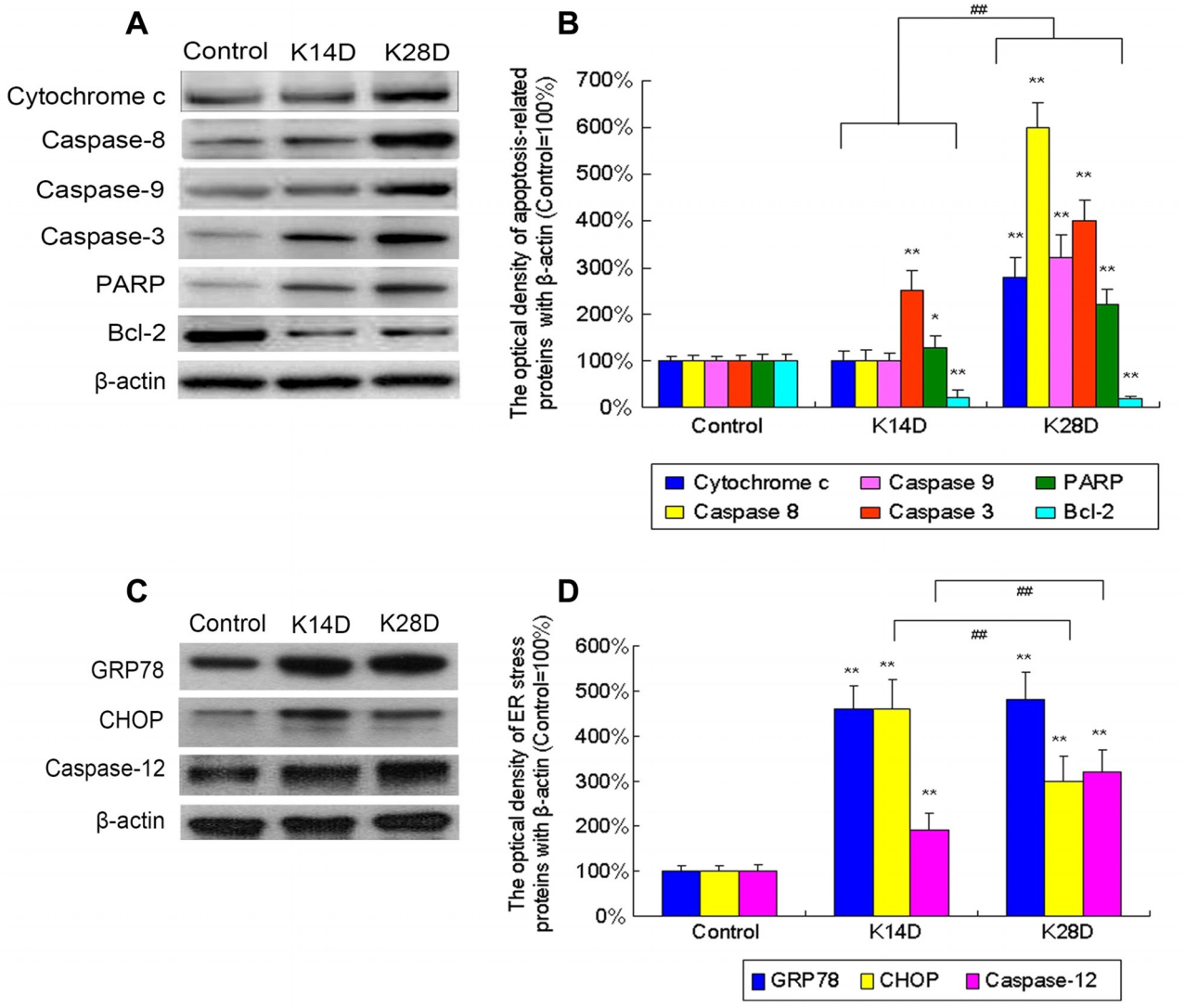

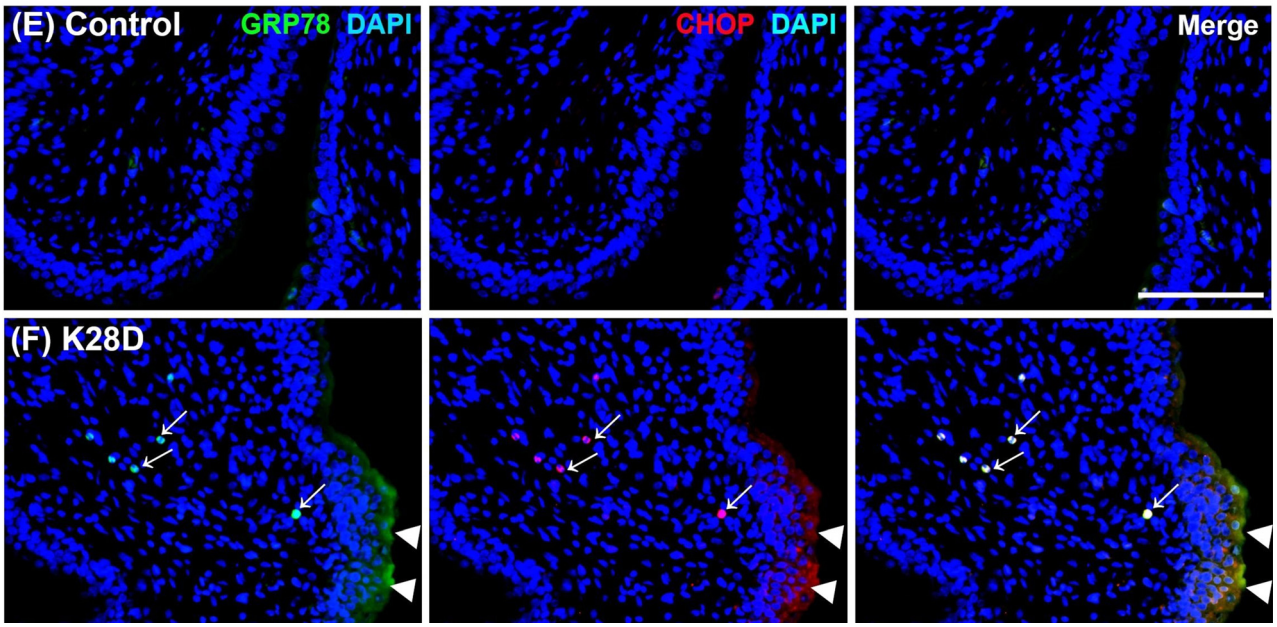

K28D groups compared with the control group. Using double-labeled immunofluoresence of GRP78 and CHOP proteins, no staining was found in the control group (Fig. 4*E*). However, after 28 days of ketamine treatment, GRP78-positive cells were colabeled with CHOP in the urothelium and suburothelium (Fig. 4*F*). These results demonstrate that ketamine-induced apoptosis was correlated with mitochondria- and ER-dependent pathways.

Effects of ketamine on expression of oxidative stress markers in the bladder. To determine the bladder oxidative damage induced by ketamine administration, expressions of DNP and nitrotyrosine were examined. As shown in Fig. 5, *A* and *B*, the expression of nitrotyrosine was 6.2-fold higher in the K14D group and 7.0-fold higher in the K28D group (Fig. 5*C*) and those of DNP and nitrotyrosine were 5.3-fold higher in the K14D and K28D groups compared with the control group (Fig. 5*B*). These findings reveal that ketamine treatment significantly increased bladder oxidative damage.

Furthermore, real time-PCR showed that mRNA expressions of antioxidant enzymes (Cu/Zn-SOD, Mn-SOD, and catalase) in the bladder were decreased after ketamine treatment (Fig. 5*C*). As shown in Fig. 5*C*, the expression of Mn-SOD was 0.60-fold in the K14D group and 0.37-fold in the K28D group (Fig. 5*C*) and those of Cu/Zn-SOD and catalase were 0.8-fold in the K14D group and 0.6-fold in the K28D group compared with the control group. Double-labeled immunofluoresence of Cu/Zn-SOD, Mn-SOD, or catalase was found in the urothelium and suburothelium in the control group (Fig. 5, *D* and *F*). Mn-SOD-positive cells colabeled with Cu/Zn-SOD-positive or catalase-positive cells were significantly decreased in the urothelium after 28 days of ketamine treatment (Fig. 5, *E* and *G*), and some inflammatory cells (arrows) in the suburothelium were costained with Cu/Zn-SOD and Mn-SOD. Such decreases in the expression levels of antioxidant enzymes implied that cellular defenses against oxidative stress declined in the ketamine-treated bladder.

Ketamine increased mitochondrial generation of ROS. The assessment of mitochondrial activity was acquired by the analysis of expressions of subunits of mitochondria respiratory enzyme complexes involving the generation of ROS. Expressions of these complexes, including NDUFS3, SDHA, UQCRC1, COX-2, and ATPB, were significantly increased in the bladder after 14 and 28 days of ketamine treatment (Fig. 6, *A* and *B*). The increase in the expression of COX-2 in the K28D group was especially more profound than that of the K14D group. This ketamine-induced increase in the expressions of mitochondria respiratory enzyme complexes suggested that ketamine caused an enhancement in the generation of ROS.

DISCUSSION

The present investigation demonstrates that ketamine administration diminished bladder volume, raised oxidative damage, increased bladder cells apoptosis, and disrupted urothelial barrier-associated protein expresisons. Such changes in morphology as well as decreases in urothelial junction proteins (E-cadherin, ZO-1, and claudin-4) in the bladder mucosa were similar to those in interstitial cystitis. Meanwhile, bladder tissues were accompanied by increases in the expressions of apoptosis-associated proteins, including cytochrome *c*, caspase-3, caspase-9, and PARP, which displayed features of mitochondria-dependent apoptotic signals, ER stress markers (GRP78, CHOP, and caspase-12), and oxidative stress markers (nitrotyrosine and DNP). Moreover, expression levels of subunits of mitochondria respiratory enzymes were significantly increased in the bladder. These findings suggest that oxidative stress mediated by mitochondria and the ER was involved in ketamine-induced bladder cell apoptosis and ulcerative cystitis.

Oxidative stress is associated with an overproduction of ROS and reactive nitrogen species. Effects of ROS on the micturation reflex have been demonstrated in several pathological conditions of the urinary bladder, such as cyclophosphamide-induced hemorrhagic cystitis, ionizing radiation cystitis, and partial bladder outlet obstruction (1, 8, 31). In the present study, the observed increase in the expressions of bladder oxidative stress markers (nitrotyrosine and DNP) suggest that oxidative stress might play a key role in the pathophysiology of KIC. Natural antioxidant mechanisms, namely, SOD and catalase, are chief defenses in cells. Cytoplasmic SOD converts superoxide to peroxide, which, in turn, is broken down by catalase to water and oxygen. If the production of the intermediate peroxide exceeds the ability of catalase to degrade it, then damages to cells can occur. Thus, it is important for SOD and catalase to work in conjunction and counterbalance. The present study shows that ketamine treatment significantly reduced expressions of antioxidant enzymes (Cu/Zn-SOD, Mn-SOD, and catalase), suggesting that ketamine enhanced ROS production by reducing antioxidant enzyme activity.

The respiratory chain of mitochondria consists of five different enzyme complexes embedded in the inner mitochondrial membrane, including NDUFS3 of complex I (NADH CoQ reductase complex), SDHA of complex II (succinate CoQ reductase complex), UQCRC1 of complex III ($CoQH_2$-cytchrome *c* reductase complex), COX-2 of complex IV (cytochrome *c* oxidase complex), and ATPB of complex V (F_0F_1 complex, ATP syntase) (37). The electrons from NADH and succinate are transferred to molecular oxygen through different redox groups bound to proteins present in the multiprotein complexes. Part of the energy released in the process is used by

Fig. 4. Alterations of expressions of apoptosis-associated proteins and endoplasmic reticulum (ER) stress markers in the bladder after ketamine administration. *A*: expression levels of proapoptotic and antiapoptotic proteins in the bladder tissue by Western blot analysis. The expression of Bcl-2 was decreased in the K14D and K28D groups. In contrast, expressions of cytochrome *c*, caspase-3, caspase-8, caspase-9, and poly(ADP-ribose) polymerase (PARP) were significantly increased in the K28D group. *B*: expression levels of 78-kDa glucose-regulated protein (GRP78), CCAAT/enhancer-binding protein homologous protein (CHOP), and caspase-12 were increased in the K14D and K28D groups. *C* and *D*: quantification of these protein expressions to β-actin. Results are normalized to the control group (equal to 100%). Values are means ± SD for $n = 8$. $^*P < 0.05$ and $^{**}P < 0.01$ vs. the control group; $^{\#\#}P < 0.01$ vs. the K14D group. *E* and *F*: immunofluorescence analysis of GRP78 and CHOP expressions after 28 days of treatment with ketamine. The arrowheads indicate GRP78-positive and CHOP-positive cells costained in the urothelium; the arrows indicate GRP78-positive and CHOP-positive cells colabeled in the suburothelium. Scale bar = 100 μm.

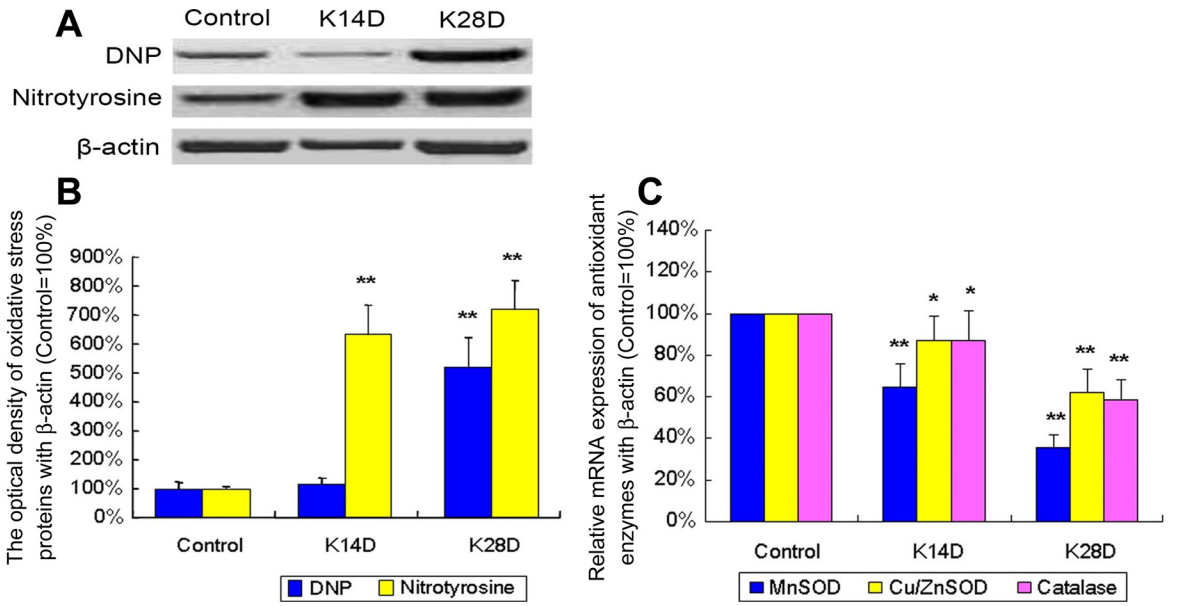

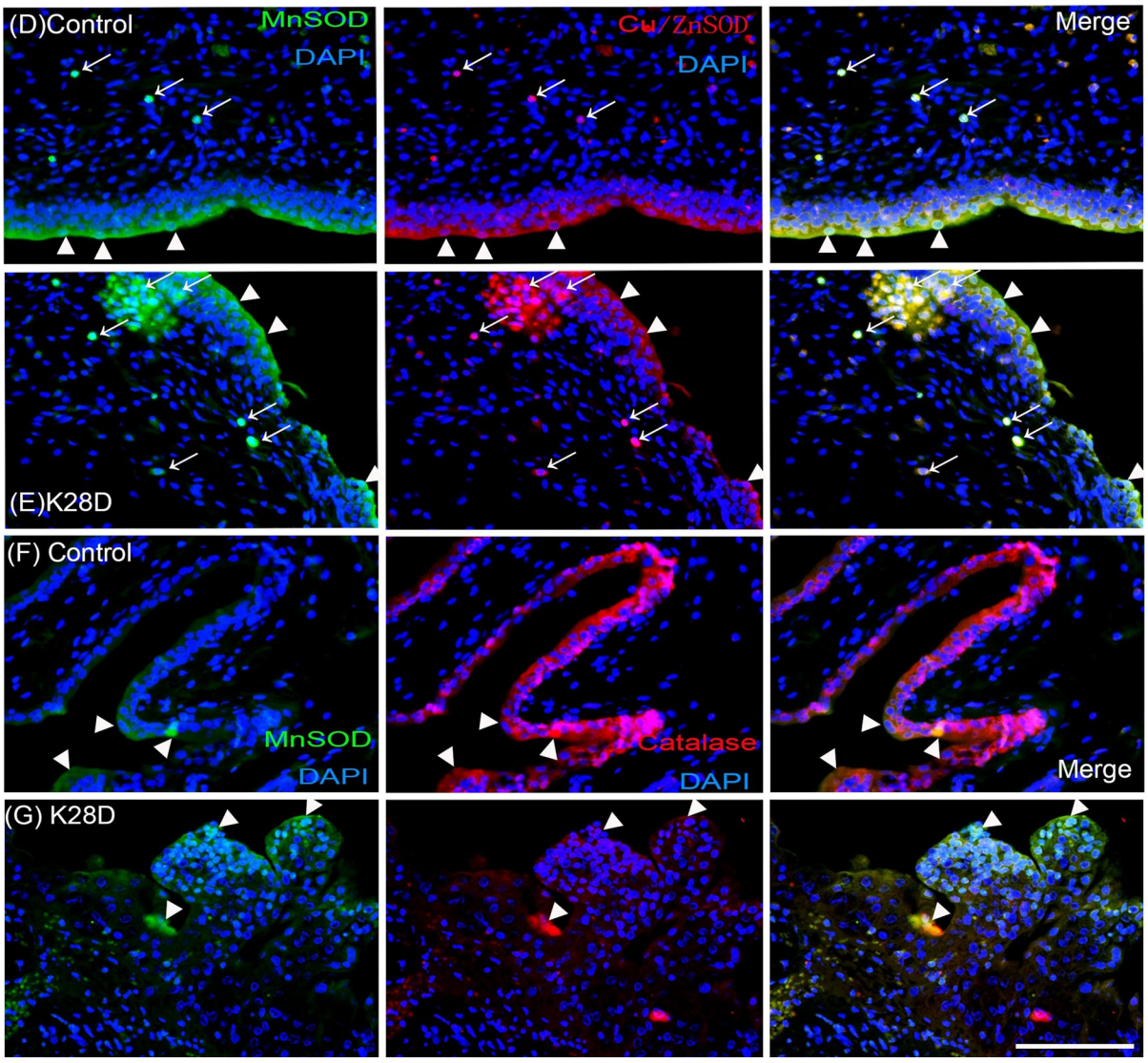

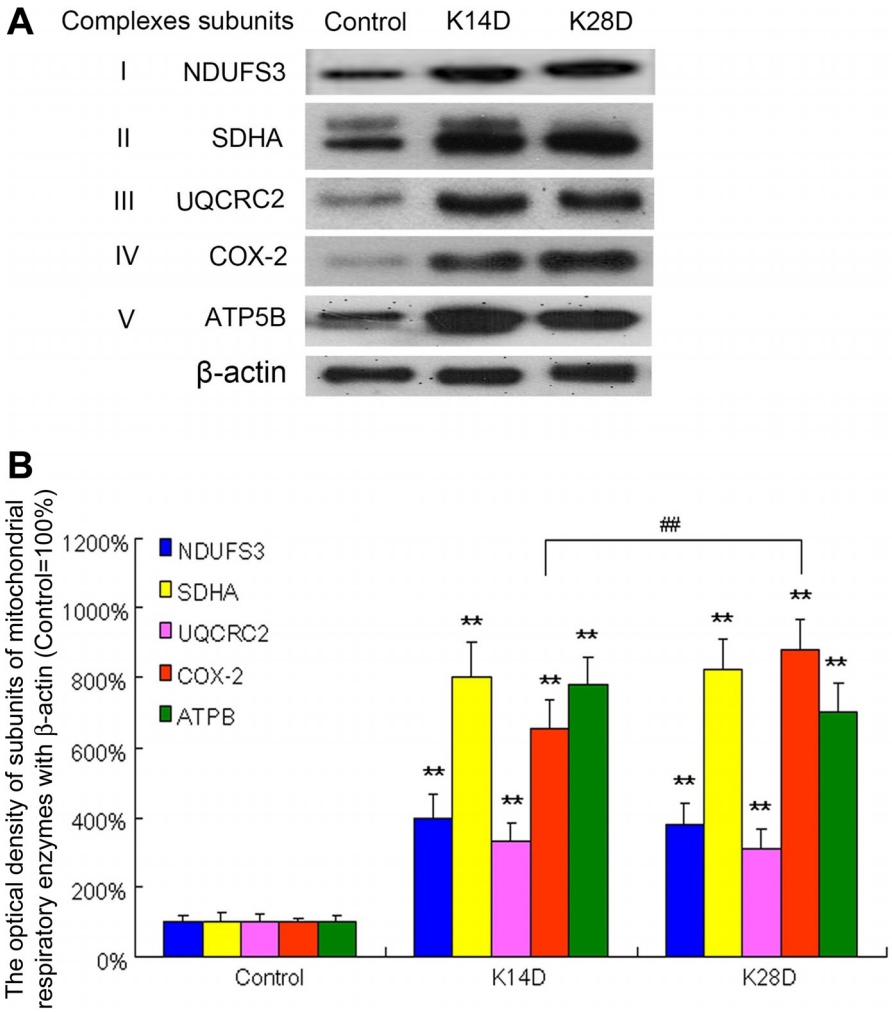

Fig. 6. Upregulation of subunits of mitochondrial respiratory enzymes after ketamine treatment. *A*: expression levels of subunits of mitochondrial respiratory enzymes [NADH dehydrogenase (ubiquinone) Fe-S protein 3 (NDUFS3) of complex I, succinate dehydrogenase complex subunit A (SDHA) of complex II, ubiquinol-cytochrome *c* reductase core protein II (UQCRC2) of complex III, cytochrome *c* oxidase (COX-2) of complex IV, and ATPB of complex V] were determined by Western blot analysis. *B*: quantification of the percentage of these mitochondrial respiratory enzymes to β-actin. Results were normalized to the control group (equal to 100%). These subunits were significantly increased in bladders treated with ketamine for 14 and 28 days. Values are means ± SD for $n = 8$. $^{**}P < 0.01$ vs. the control group; $^{\#\#}P < 0.01$ vs. the K14D group.

complexes I, III, and IV to pump H^+ to the intermembrane space, generating an electrochemical H^+ gradient through the mitochondrial inner membrane. This electrochemical H^+ gradient drives proton flux back to the mitochondria through ATP synthase (complex V), which is coupled to the synthesis of ATP (4). The present study showed overexpressions of all five of these respiratory enzyme complexes after 28 days of ketamine injection. When the mitochondrial respiration chain provides ATP for bladder hyperactivity, an increase in the generation of ROS in cells can occur by increasing electron leakage from respiratory enzyme complexes of mitochondria (28, 35). In patients with multiple sclerosis, a significant increase in all respiratory complex activities has been observed. Mitochondrial lipid peroxidation and mitochondrial SOD1 overexpressions were also detected, showing that changes in mitochondrial aerobic metabolism is important in some neurodegenerative diseases (26). In a previous investigation (36), urothelial biopsies from patients with IC/PBS were reported to release more ATP in response to stretch or EFS than those from normal bladder urothelial biopsies.

The bladder urothelium plays a crucial role as a barrier between urine and bladder stroma. The barrier is thought to result from the formation of intracellular and intercellular junctions, which include adherens junction and tight junctions. Tight junctions are expressed in umbrella cells and include ZO-1, occludin, and claudin families. Adherent junctions occur at cell-cell junctions, which are more basal than tight junctions. E-cadherin is known to be crucial to intercellular homophilic Ca^{2+}-dependent adhesion. A previous study (52) has reported a decrease in E-cadherin expression in IC patients with higher visceral pain scores. Urothelial lining defects also play an important role in bladder oversensitivity (21). Moreover, it has

Fig. 5. Effects of ketamine administration on expressions of oxidative stress markers and antioxidant enzymes in the bladder. *A* and *B*: expression levels of oxidative stress markers [2,4-dinitrophenol (DNP) and nitrotyrosine] by Western blot analysis. *C*: antioxidant enzymes [Mn-SOD (SOD2), Cu/Zn-SOD (SOD1), and catalase] determined by RT-PCR in the three different groups. Quantification of the percentages of these proteins to β-actin are shown. Results were normalized to the control group (equal to 100%). Values are means ± SD for $n = 8$. $^{*}P < 0.05$ and $^{**}P < 0.01$ vs. the control group. *D–G*: immunofluorescence analysis of Mn-SOD, Cu/Zn-SOD, and catalase expressions after treatment with ketamine. The arrowheads indicate Mn-SOD-positive and Cu/Zn-SOD-positive cells or Mn-SOD-positive and catalase-positive cells costained in the urothelium, and the arrows indicate cells colabeled in the suburothelium. Scale bar = 100 μm.

been reported that a decrease in expression of ZO-1 and occludin could result in an increase in epithelial paracellular permeability in IC/PBS patients (59). In the present study, we showed a decrease in urothelium thickness with disruption of urothelial E-cadherin and tight junction-associated proteins (ZO-1 and claudin-4) and the ulcerated urothelium after ketamine administration. The significance of such a decrease in E-cadherin and tight junction protein expressions in the epithelial permeability of the bladder of ketamine addicts requires further evaluation.

The central components of apoptosis are a group of proteolytic enzymes called caspases, which can be activated by various types of stimulation. Loss of mitochondrial membrane potential and release of cytochrome *c* are key events in initiating mitochondria-involved apoptosis (5). The released cytochrome *c* activates caspase-9, which consequently induces caspase-3 activation, resulting in the cleavage of several cellular proteins, finally leading to apoptosis. In adddition, an ER stress-triggered caspase cascade, involving caspase-3 and caspase-8, plays an important role in ketamine-induced bladder apoptosis. ER stress-induced apoptosis also involves CHOP and caspase-8-mediated cleavage of Bap31 to Bap 21 and propagates apoptotic signals from the ER to mitochondria. The present study revealed a significant increase in the expressions of caspase-3, caspase-8, caspase-9, cytochrome *c*, and PARP as well as TUNEL-positive cells in bladder tissue after ketamine treatment, especially after 28 days of treatment. In addition, ketamine-induced apoptosis was accompanied by a significant increase in oxidative stress markers (nitrotyrosine and DNP), ER-associated apoptosis protein CHOP, and subunits of mitochondrial respiratory complexes. Our findings suggest that ketamine-induced bladder apoptosis involves oxidative stress mediated by both mitochondrial and ER pathways.

The present results suggest that urothelial barrier damage and apoptosis as well as ulcerative cystitis after ketamine administration are associated with an effect of ketamine and/or its metabolites on the bladder. It is possible that an indirect effect may also occur by causing macrophage activation and resulting in apoptosis of the DSM and interstitium due to the circulation of ketamine or its metabolites. At the present time, it is still unclear whether the generation of ROS and apoptosis/ER stress are a direct or an indirect effect of ketamine. The information obtained in the present study is useful in providing valuable insights into blocking the urinary effects of ketamine. We intend to further explore this issue in our future investigations.

In conclusion, the present study demonstrates that ketamine enhances the generation of ROS mediated by mitochondria and the ER, leading to the inducement of oxidative stress with accompanying urothelial lining defects and consequently enhancing bladder apoptosis. Such effects on the urothelial barrier as well as increased oxidative stress and apoptosis are potential factors underlying bladder overactivity and the inflammatory process in KIC.

ACKNOWLEDGMENTS

The authors are grateful to Prof. Chang-Hwei Chen (University at Albany, State University of New York) for valuable comments on this manuscript.

GRANTS

This work was supported by Ministry of Health and Welfare, Executive Yuan Grant MOHW103-TD-B-111-05, in part by Department of Medical Research, Kaohsiung Medical University Hospital Grants KMUH101-1R43 and KMUH 102-2R41, Kaohsiung Municipal Hsiao-Kang Hospital Grants Kmhk-100-025, Kmhk-101-016, and Kmhk-101-017, and Ministry of Science and Technology (NSC-102-2314-B-037-049; MOST 103-2314-B-037-058-MY2).

DISCLOSURES

No conflicts of interest, financial or otherwise, are declared by the author(s).

AUTHOR CONTRIBUTIONS

Author contributions: K.-M.L., S.-M.C., C.L., and Y.-S.J. conception and design of research; K.-M.L. and Y.-S.J. analyzed data; K.-M.L., C.L., W.-J.W., and Y.-S.J. edited and revised manuscript; S.-M.C. prepared figures; S.-M.C., W.-J.W., and Y.-S.J. approved final version of manuscript; Y.-L.L., R.-J.L., and M.-Y.J. interpreted results of experiments; C.-C.W., M.-C.L., J.-H.L., and W.-T.H. performed experiments; W.-T.H. and Y.-S.J. drafted manuscript.

REFERENCES

1. **Abraham P, Rabi S, Selvakumar D.** Protective effect of aminoguanidine against oxidative stress and bladder injury in cyclophosphamide-induced hemorrhagic cystitis in rat. *Cell Biochem Funct* 27: 56–62, 2009.
2. **Aikawa K, Leggett R, Levin RM.** Effect of age on hydrogen peroxide mediated contraction damage in the male rat bladder. *J Urol* 170: 2082–2085, 2003.
3. **Andersson KE, Arner A.** Urinary bladder contraction and relaxation: physiology and pathophysiology. *Physiol Rev* 84: 935–986, 2004.
4. **Bornstein B, Huertas R, Ochoa P, Campos Y, Guillen F, Garesse R, Arenas J.** Mitochondrial gene expression and respiratory enzyme activities in cardiac diseases. *Biochim Biophys Acta* 1406: 85–90, 1998.
5. **Budd SL, Tenneti L, Lishnak T, Lipton SA.** Mitochondrial and extramitochondrial apoptotic signaling pathways in cerebrocortical neurons. *Proc Natl Acad Sci USA* 97: 6161–6166, 2000.
6. **Cannon TW, Damaser MS.** Effects of anesthesia on cystometry and leak point pressure of the female rat. *Life Sci* 69: 1193–1202, 2001.
7. **Chen WC, Hayakawa S, Shimizu K, Chien CT, Lai MK.** Catechins prevents substance P-induced hyperactive bladder in rats via the down-regulation of ICAM and ROS. *Neurosci Lett* 367: 213–217, 2004.
8. **Chiba K, Yamaguchi K, Ando M, Miyake H, Fujisawa M.** Expression pattern of testicular claudin-11 in infertile men. *Urology* 80: 1161 e1113–1167, 2012.
9. **Chien CT, Yu HJ, Lin TB, Lai MK, Hsu SM.** Substance P via NK1 receptor facilitates hyperactive bladder afferent signaling via action of ROS. *Am J Physiol Renal Physiol* 284: F840–F851, 2003.
10. **Chiew YW, Yang CS.** Disabling frequent urination in a young adult. Ketamine-associated ulcerative cystitis. *Kidney Int* 76: 123–124, 2009.
11. **Chu PS, Ma WK, Wong SC, Chu RW, Cheng CH, Wong S, Tse JM, Lau FL, Yiu MK, Man CW.** The destruction of the lower urinary tract by ketamine abuse: a new syndrome? *BJU Int* 102: 1616–1622, 2008.
12. **Chuang SM, Liu KM, Lee YC, Lin RJ, Chang CY, Wu WJ, Chang WC, Levin RM, Juan YS.** Effects of supraphysiological testosterone treatment and orchiectomy on ischemia/reperfusion-induced bladder dysfunction in male rabbits. *J Sex Med* 10: 1278–1290, 2013.
13. **Chuang SM, Liu KM, Li YL, Jang MY, Lee HH, Wu WJ, Chang WC, Levin RM, Juan YS.** Dual involvements of cyclooxygenase and nitric oxide synthase expressions in ketamine-induced ulcerative cystitis in rat bladder. *Neurourol Urodyn* 32: 1137–1143, 2013.
16. **Cockayne DA, Hamilton SG, Zhu QM, Dunn PM, Zhong Y, Novakovic S, Malmberg AB, Cain G, Berson A, Kassotakis L, Hedley L, Lachnit WG, Burnstock G, McMahon SB, Ford AP.** Urinary bladder hyporeflexia and reduced pain-related behaviour in P2X3-deficient mice. *Nature* 407: 1011–1015, 2000.
17. **Cottrell A, Warren K, Ayres R, Weinstock P, Kumar V, Gillatt D.** The destruction of the lower urinary tract by ketamine abuse: a new syndrome? *BJU Int* 102: 1178–1179, 2008.
18. **de Jongh R, Haenen GR, van Koeveringe GA, Dambros M, De Mey JG, van Kerrebroeck PE.** Oxidative stress reduces the muscarinic receptor function in the urinary bladder. *Neurourol Urodyn* 26: 302–308, 2007.
19. **Erdem E, Leggett R, Dicks B, Kogan BA, Levin RM.** Effect of bladder ischaemia/reperfusion on superoxide dismutase activity and contraction. *BJU Int* 96: 169–174, 2005.
20. **Fiksdal L, Tryland I.** Application of rapid enzyme assay techniques for monitoring of microbial water quality. *Curr Opin Biotechnol* 19: 289–294, 2008.

21. **Graham E, Chai TC.** Dysfunction of bladder urothelium and bladder urothelial cells in interstitial cystitis. *Curr Urol Rep* 7: 440–446, 2006.
22. **Green DR, Kroemer G.** The pathophysiology of mitochondrial cell death. *Science* 305: 626–629, 2004.
23. **Gupta GN, Lu SG, Gold MS, Chai TC.** Bladder urothelial cells from patients with interstitial cystitis have an increased sensitivity to carbachol. *Neurourol Urodyn* 28: 1022–1027, 2009.
24. **Herrera GM, Meredith AL.** Diurnal variation in urodynamics of rat. *PLos One* 5: e12298, 2010.
25. **Hitomi J, Katayama T, Eguchi Y, Kudo T, Taniguchi M, Koyama Y, Manabe T, Yamagishi S, Bando Y, Imaizumi K, Tsujimoto Y, Tohyama M.** Involvement of caspase-4 in endoplasmic reticulum stress-induced apoptosis and Aβ-induced cell death. *J Cell Biol* 165: 347–356, 2004.
26. **Inarrea P, Alarcia R, Alava MA, Capablo JL, Casanova A, Iniguez C, Iturralde M, Larrode P, Martin J, Mostacero E, Ara JR.** Mitochondrial complex enzyme activities and cytochrome C expression changes in multiple sclerosis. *Mol Neurobiol* 49: 1–9, 2014.
27. **Jang MY, Long CY, Chuang SM, Huang CH, Lin HY, Wu WJ, Juan YS.** Sexual dysfunction in women with ketamine cystitis: a case-control study. *BJU Int* 110: 427–431, 2012.
28. **Jastroch M, Divakaruni AS, Mookerjee S, Treberg JR, Brand MD.** Mitochondrial proton and electron leaks. *Essays Biochem* 47: 53–67, 2010.
29. **Juan YS, Chuang SM, Lee YL, Long CY, Wu TH, Chang WC, Levin RM, Liu KM, Huang CH.** Green tea catechins decrease oxidative stress in surgical menopause-induced overactive bladder in a rat model. *BJU Int* 110: E236–244, 2012.
30. **Juan YS, Hydery T, Mannikarottu A, Kogan B, Schuler C, Leggett RE, Lin WY, Huang CH, Levin RM.** Coenzyme Q10 protect against ischemia/reperfusion induced biochemical and functional changes in rabbit urinary bladder. *Mol Cell Biochem* 311: 73–80, 2008.
31. **Juan YS, Lin WY, Kalorin C, Kogan BA, Levin RM, Mannikarottu A.** The effect of partial bladder outlet obstruction on carbonyl and nitrotyrosine distribution in rabbit bladder. *Urology* 70: 1249–1253, 2007.
32. **Juan YS, Mannikarottu A, Schuler C, Lin WY, Huang CH, Levin RM.** The immediate effect of nitric oxide on the rabbit bladder after ovariectomy. *Nitric Oxide Biol Chem* 19: 289–294, 2008.
33. **Keay S, Seillier-Moiseiwitsch F, Zhang CO, Chai TC, Zhang J.** Changes in human bladder epithelial cell gene expression associated with interstitial cystitis or antiproliferative factor treatment. *Physiol Genomics* 14: 107–115, 2003.
34. **Kim R, Emi M, Tanabe K, Murakami S.** Role of the unfolded protein response in cell death. *Apoptosis* 11: 5–13, 2006.
35. **Kirkinezos IG, Moraes CT.** Reactive oxygen species and mitochondrial diseases. *Semin Cell Dev Biol* 12: 449–457, 2001.
36. **Kumar V, Chapple CR, Surprenant AM, Chess-Williams R.** Enhanced adenosine triphosphate release from the urothelium of patients with painful bladder syndrome: a possible pathophysiological explanation. *J Urol* 178: 1533–1536, 2007.
37. **Lee CH, Wu SB, Hong CH, Liao WT, Wu CY, Chen GS, Wei YH, Yu HS.** Aberrant cell proliferation by enhanced mitochondrial biogenesis via mtTFA in arsenical skin cancers. *Am J Pathol* 178: 2066–2076, 2011.
38. **Lee HC, Wei YH.** Mitochondrial biogenesis and mitochondrial DNA maintenance of mammalian cells under oxidative stress. *Int J Biochem Cell Biol* 37: 822–834, 2005.
39. **Lee WC, Chiang PH, Tain YL, Wu CC, Chuang YC.** Sensory dysfunction of bladder mucosa and bladder oversensitivity in a rat model of metabolic syndrome. *PLos One* 7: e45578, 2012.
40. **Lee WC, Chuang YC, Chiang PH, Chien CT, Yu HJ, Wu CC.** Pathophysiological studies of overactive bladder and bladder motor dysfunction in a rat model of metabolic syndrome. *J Urol* 186: 318–325, 2011.
41. **Lin AT, Yang CH, Chen KK, Chang LS.** Detrusor mitochondrial lipid peroxidation and superoxide dismutase activity in partial bladder outlet obstruction of rabbits. *Neurourol Urodyn* 24: 282–287, 2005.
42. **Liu HT, Shie JH, Chen SH, Wang YS, Kuo HC.** Differences in mast cell infiltration, E-cadherin, and zonula occludens-1 expression between patients with overactive bladder and interstitial cystitis/bladder pain syndrome. *Urology* 80: 225 e213–228, 2012.
43. **Louisiriotchanakul S, Thongput A, Khamboonruang C, Taylor GP, Kunstadter P, Wasi C.** No evidence of HTLV-I or HTLV-II infection among the Hmong people of northern Thailand or injecting drug users in Bangkok. *J Acquir Immune Defic Syndr Hum Retrovirol* 23: 441–442, 2000.
44. **Mason K, Cottrell AM, Corrigan AG, Gillatt DA, Mitchelmore AE.** Ketamine-associated lower urinary tract destruction: a new radiological challenge. *Clin Radiol* 65: 795–800, 2010.
45. **Masuda H, Kihara K, Saito K, Matsuoka Y, Yoshida S, Chancellor MB, de Groat WC, Yoshimura N.** Reactive oxygen species mediate detrusor overactivity via sensitization of afferent pathway in the bladder of anaesthetized rats. *BJU Int* 101: 775–780, 2008.
46. **Meng E, Chang HY, Chang SY, Sun GH, Yu DS, Cha TL.** Involvement of purinergic neurotransmission in ketamine induced bladder dysfunction. *J Urol* 186: 1134–1141, 2011.
47. **Ott M, Gogvadze V, Orrenius S, Zhivotovsky B.** Mitochondria, oxidative stress and cell death. *Apoptosis* 12: 913–922, 2007.
48. **Parekh MH, Lobel R, O'Connor LJ, Leggett RE, Levin RM.** Protective effect of vitamin E on the response of the rabbit bladder to partial outlet obstruction. *J Urol* 166: 341–346, 2001.
49. **Parkin MC, Turfus SC, Smith NW, Halket JM, Braithwaite RA, Elliott SP, Osselton MD, Cowan DA, Kicman AT.** Detection of ketamine and its metabolites in urine by ultra high pressure liquid chromatography-tandem mass spectrometry. *J Chromatogr B Analyt Technol Biomed Life Sci* 876: 137–142, 2008.
50. **Sakamoto S.** Synaptic weight normalization effects for topographic mapping formation. *Neural Networks* 17: 1109–1120, 2004.
51. **Shahani R, Streutker C, Dickson B, Stewart RJ.** Ketamine-associated ulcerative cystitis: a new clinical entity. *Urology* 69: 810–812, 2007.
52. **Shie JH, Kuo HC.** Higher levels of cell apoptosis and abnormal E-cadherin expression in the urothelium are associated with inflammation in patients with interstitial cystitis/painful bladder syndrome. *BJU Int* 108: E136–E141, 2011.
53. **Sun Y, Chen M, Lowentritt BH, Van Zijl PS, Koch KR, Keay S, Simard JM, Chai TC.** EGF and HB-EGF modulate inward potassium current in human bladder urothelial cells from normal and interstitial cystitis patients. *Am J Physiol Cell Physiol* 292: C106–C114, 2007.
54. **Tagawa Y, Hiramatsu N, Kasai A, Hayakawa K, Okamura M, Yao J, Kitamura M.** Induction of apoptosis by cigarette smoke via ROS-dependent endoplasmic reticulum stress and CCAAT/enhancer-binding protein-homologous protein (CHOP). *Free Radic Biol Med* 45: 50–59, 2008.
55. **Tsai JH, Tsai KB, Jang MY.** Ulcerative cystitis associated with ketamine. *Am J Addict* 17: 453, 2008.
56. **Tsai TH, Cha TL, Lin CM, Tsao CW, Tang SH, Chuang FP, Wu ST, Sun GH, Yu DS, Chang SY.** Ketamine-associated bladder dysfunction. *Int J Urol* 16: 826–829, 2009.
57. **Yu HJ, Chien CT, Lai YJ, Lai MK, Chen CF, Levin RM, Hsu SM.** Hypoxia preconditioning attenuates bladder overdistension-induced oxidative injury by up-regulation of Bcl-2 in the rat. *J Physiol* 554: 815–828, 2004.
58. **Yuan JS, Reed A, Chen F, Stewart CN Jr.** Statistical analysis of real-time PCR data. *BMC Bioinform* 7: 85, 2006.
59. **Zhang CO, Wang JY, Koch KR, Keay S.** Regulation of tight junction proteins and bladder epithelial paracellular permeability by an antiproliferative factor from patients with interstitial cystitis. *J Urol* 174: 2382–2387, 2005.